Pacific Northwest
NATIONAL LABORATORY

PNNL-32425

Laser Surface Processing of Alloys for Corrosion Protection

Final Project Report of Marine Energy Seedling Project

January 2022

Aashish Rohatgi (aashish.rohatgi@pnnl.gov)
George Bonheyo (george.bonheyo@pnnl.gov)

U.S. DEPARTMENT OF ENERGY

Prepared for the U.S. Department of Energy
under Contract DE-AC05-76RL01830

DISCLAIMER

This report was prepared as an account of work sponsored by an agency of the United States Government. Neither the United States Government nor any agency thereof, nor Battelle Memorial Institute, nor any of their employees, makes **any warranty, express or implied, or assumes any legal liability or responsibility for the accuracy, completeness, or usefulness of any information, apparatus, product, or process disclosed, or represents that its use would not infringe privately owned rights**. Reference herein to any specific commercial product, process, or service by trade name, trademark, manufacturer, or otherwise does not necessarily constitute or imply its endorsement, recommendation, or favoring by the United States Government or any agency thereof, or Battelle Memorial Institute. The views and opinions of authors expressed herein do not necessarily state or reflect those of the United States Government or any agency thereof.

PACIFIC NORTHWEST NATIONAL LABORATORY
operated by
BATTELLE
for the
UNITED STATES DEPARTMENT OF ENERGY
under Contract DE-AC05-76RL01830

Printed in the United States of America

Available to DOE and DOE contractors from the
Office of Scientific and Technical Information,
P.O. Box 62, Oak Ridge, TN 37831-0062;
ph: (865) 576-8401
fax: (865) 576-5728
email: reports@adonis.osti.gov

Available to the public from the National Technical Information Service
5301 Shawnee Rd., Alexandria, VA 22312
ph: (800) 553-NTIS (6847)
email: orders@ntis.gov <https://www.ntis.gov/about>
Online ordering: http://www.ntis.gov

PNNL-32425

Laser Surface Processing of Alloys for Corrosion Protection

Final Project Report of Marine Energy Seedling Project

January 2022

Aashish Rohatgi (aashish.rohatgi@pnnl.gov)
George Bonheyo (george.bonheyo@pnnl.gov)

Prepared for
the U.S. Department of Energy
under Contract DE-AC05-76RL01830

Pacific Northwest National Laboratory
Richland, Washington 99354

Executive Summary

This work was undertaken as part of a Seedling project funded by the Marine Energy Program within the DOE's Water Power Technology Office. The goal of this work was to explore surface modification of commercial alloys to enhance their corrosion resistance in marine environments. Existing corrosion protection solutions such as painting/coatings, or using corrosion resistant materials, suffer from durability issues and/or are expensive. Therefore, laser surface processing (LSP) was proposed as an alternate, and a novel, corrosion protection technique that can potentially overcome the challenges of existing techniques.

Laser surface processing employs relatively low (~hundreds of mJ) energy laser pulses to locally modify the surface of the given material. In this project, LSP was used to surface modify test coupons of 6061-T6 aluminum (Al) alloy, low-carbon steel and 316 stainless steel. Bench-top, limited-term corrosion tests were performed on LSP-modified and un-modified samples and their respective corrosion behavior was analyzed through gravimetry, surface roughness measurements and x-ray photoelectron spectroscopy. Based on these tests, the key observations are:

- 6061-T6 Al shows up to ~15% improved corrosion resistance relative to non-LSP'ed samples.
- Low-carbon steel shows up to ~25% improved corrosion resistance relative to non-LSP'ed samples.
- Laser power used for LSP needs to be controlled to achieve the necessary corrosion protection of the modified surfaces.

These initial results show LSP to be a promising technique for corrosion protection, specially as it avoids the need for paints/coatings that otherwise can leach into the ocean. As LSP can be applied locally, and in a desired location without affecting the remainder of the material, its applicability at joints and welds, of components and structures should be explored. Additional effort is needed to fully understand the corrosion protection mechanism(s) in LSP'ed surfaces and to evaluate their performance in long-duration tests in marine environments. Determining the suitability of LSP for protecting large structures will also be valuable for marine energy applications.

Acknowledgments

We would like to acknowledge Prof. Hongtao Ding and his team at the University of Iowa for their help in fabricating laser processed samples. We would also like to acknowledge the following PNNL staff for their help in executing this project: Robert Seffens (corrosion testing and sample handling), Morotolaoluwa (Tola) Alabi and Saumyadeep Jana (literature review and initial testing), Hong (Amy) Qiao for surface profilometry and Mark Engelhard for XPS. A portion of this research was performed using facilities at the Environmental Molecular Sciences Laboratory, a national scientific user facility sponsored by the U.S. Department of Energy's (DOE's) Office of Biological and Environmental Research and located at PNNL. PNNL is a multiprogram national laboratory operated by Battelle for the DOE under Contract DEAC05-76RL01830.

Acronyms and Abbreviations

Ag	Silver
Al	Aluminum
Al_2O_3	Alumina
Al_4C_3	Aluminum carbide
Ar	Argon
ASM	American Society for Metals
ASTM	American Society for Testing and Materials
C	Carbon
CO_2	Carbon dioxide
Cr	Chromium
DOD	Department of Defense
DOE	Department of Energy
$FeCl_3$	Ferric chloride
FWHM	Full-width half maximum
GAO	Government Accountability Office
LSP	Laser surface processing
Mg	Magnesium
MS&T	Materials Science and Technology
NaCl	Sodium chloride
Nd:YAG	Neodymium-doped yttrium aluminum garnet
Ni	Nickel
ONR	Office of Naval Research
PI	Principal investigator
PNNL	Pacific Northwest National Laboratory
RTV	Room-temperature vulcanizing
Rq	Room mean square roughness
SiO_2	Silicon dioxide
SS	Stainless steel
TRL	Technology readiness level
UV	ultra-violet
VCI	Vapor corrosion inhibitors
XPS	X-ray photoelectron spectroscopy

Contents

Figures

1.0 Background

This work was undertaken as part of a Seedling project funded by the Marine Energy Program within the DOE's Water Power Technology Office. The goal of this work was to explore surface modifications of existing commercial alloys to enhance their corrosion resistance in marine environments. Corrosion in marine environments is a long-standing problem and the traditional corrosion protection approaches typically involve painting/coating and/or using expensive duplex/super duplex stainless steel (SS). However, polymer based coatings have durability issues and need to be reapplied periodically, incurring overhead and maintenance costs. Thus, this Seedling project was proposed with the goal of exploring laser surface processing (LSP) as a novel corrosion protection technique. LSP does not involve paints/coatings and may enhance corrosion resistance of low-cost materials. Therefore, LSP has the potential as an alternative corrosion protection technique that can alleviate some of the durability and cost challenges of existing corrosion protection approaches.

Laser surface processing employs relatively low (~hundreds of mJ) energy laser pulses to locally modify the surface of the given material. Localized surface modification of materials, without having a direct impact on their bulk properties, can be realized by numerous conventional surface-engineering approaches including electrodeposition, physical and chemical vapor depositions, thermal and plasma spraying, and organic polymeric coatings. In a recent work published by one of the PIs (AR), LSP was shown to significantly enhance the corrosion resistance of a magnesium (Mg) AZ31B alloy in salt water [Jana et al., 2021]. This encouraging result in Mg raised an interesting possibility if similar corrosion protection could also be achieved in aluminum (Al) and steel alloys, specifically those that are used in marine environments. Therefore, this seedling was undertaken to explore the corrosion behavior of laser surface processed 6061 Al alloy and steels.

2.0 Literature Review

2.1 Corrosion Challenges in the Navy and the Protection Techniques

Scope of the problem: Corrosion is a big challenge for the US department of defense (DOD) both from a cost perspective as well as defense readiness, and has been a subject of government accountability office (GAO) reports [GAO Report]. Since both, navy ships and marine energy devices, operate in marine environments, they likely face similar corrosion issues. The US Navy corrosion costs are estimated to be ~3 Billion/year [News Report-Millitary.com]. In fact, the U.S. Office of Naval Research (ONR) has a special office that focuses on solving corrosion challenges for the US Navy [ONR Departments]. Navy ships typically go to a dry dock every 5-7 years for repairs and maintenance including paint restoration while freight transport ships usually go 5 years between dry dock sessions. Locations that need to be protected against corrosion include ship hulls (interior and exterior), decks, tanks (ballast and wastewater) and voids (cavities in hull walls) – these are typically steel structures. Corrosion can also happen where paint gets damaged (e.g. where the anchor bumps against the hulls), at the waterline, etc. Galvanic corrosion can also happen when dissimilar materials (e.g. steel and titanium, or steel and aluminum) components come in contact. Crevice corrosion can come into play around joints and fasteners. These corrosion scenarios, such as corrosion at the waterline, galvanic corrosion, and crevice corrosion are also relevant to DOE's Marine Energy program.

Corrosion protection methods: Corrosion protection for ships' structure is primarily accomplished using coatings, and cathodic protection. See Fig. 1 schematic below.

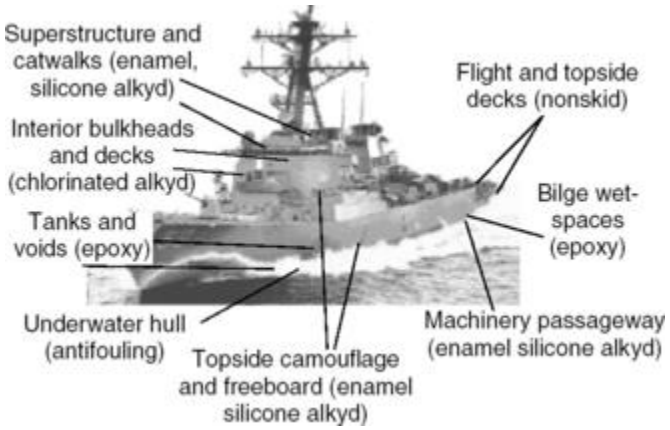

Figure 1: A variety of organic coatings for interior and exterior applications are used on ships for corrosion protection and this schematic shows the type of coatings, and locations where they are used on the ships [ASM International Handbook].

Paints are used on hulls and tanks. On the bottom of ship hulls, a special epoxy-based red paint is used to prevent rust and limit barnacle growth, and the color helps to differentiate the underwater hull from the above-water hull. The lifespan of epoxy coatings is less than 3 years, but new advanced high-solid epoxy coatings have increased lifespans of almost 10 years (e.g. USS Ogden) [ASM International Handbook]. For Naval aircraft, coatings are also the most used approach for corrosion prevention. Repainting is time consuming: Rust must be removed; preparation and painting is done while on the ship and in the dry dock, and it requires protective clothing and breathing apparatus. Some of these paints can be expensive(~Ameron PSX-700

retails at ~$250/gallon) [Popular Mechanics Article]. While paints for marine energy devices do not need to meet military standards, some coatings are even more expensive (e.g., Intersleek 1100SR retails at ~$900/gal) and the labor and costs associated with scraping off the existing rust and efforts to repaint can be expected in marine energy devices as well.

Coatings entail pre-treatments such as chemical conversion coating/anodizing on Al and phosphate coatings on steels. These serve as corrosion inhibitors and prepare the surface for the next layers. The next layer consists of epoxy polyimide containing corrosion-inhibitor additives and the final layer is a topcoat of polyurethane containing filler materials for protection against UV/radiation. Sealants are used around joints and fasteners; these sealants are adhesives and corrosion-inhibiting compounds in the form of paste, rope or tape. In most applications, polysulfide or room-temperature vulcanizing (RTV) elastomeric sealant, polythioether, and fluorinated resins such as Skyflex (W.L. Gore & Associates, Inc.) are commonly used [ASM International Handbook]. Other strategies for corrosion prevention include water displacing products, typically petroleum-based light oils and thixotropic greases, desiccants and dehumidification. In closed environments, such as electronic components in military and navy platforms, vapor corrosion inhibitors (VCI) are used. These have high vapor pressure, allowing them to volatilize, and then get adsorbed onto the metallic surface to prevent corrosion [VCI Inhibitors].

Non-coating based corrosion protection approaches include material substitution. For example, 7075-T6 and 2024-T3 are used for their high strength but have poor corrosion resistance. Therefore, these alloys are being replaced by newer corrosion-resistant alloys or existing alloys with different heat-treatment tempers e.g. 7055-T7751, 7150-T77511, 2224-T3511, 2324-T39, and 2525-T3. These alloy-tempers have higher thresholds to stress corrosion cracking, corrosion fatigue and intergranular and pitting corrosion. If alloy substitution is cost prohibitive, in-situ heat-treatments can be performed. However, while such heat-treatments are conceptually feasible, performing them in the field and in-situ can be challenging. Field application of these heat-treatments require tailoring for each sub-component and location to take into account the required heating and cooling cycles while still being connected to the remainder of the structure and components. For marine energy applications, in-field heat-treatment will require innovative approaches and is an interesting opportunity of new research.

2.2 Commercial Laser Systems

To date, PNNL's work on the use of LSP for surface protection has been done using a Nd:YAG laser system in a collaborator's research lab and it is not known a priori if other types of lasers would be equally effective for surface protection. At the lower end of energy (10's W to 100 W), laser system (e.g. those sold by www.Laserstar.net) for surface marking can cost between $30K-$100K. At the higher energy end, for example, PNNL recently purchased a laser system with a 2 kW Ytterbium fiber laser with ~ 2 ft. x ~1 ft. x ~1 ft. x-y-z travel and maximum velocity (x-y) of 5 m/s. The base system is ~$ 275K and may require additional $30K-$50K worth of optics suitable to perform surface treatments.

2.3 Literature on Laser Processing of 6061 Al

In general, Al alloys in peak-strength temper have poorer corrosion resistance than those with a lower strength temper. Therefore, for a given Al alloy, localized heating (and melting, followed by rapid solidification) due to laser treatment is expected to modify the local temper and affect the corrosion behavior relative to the base metal. Al has poor absorption of electromagnetic

radiation due to high density of free electrons but it seems to be 3x more absorptive to Nd:YAG laser wavelength (1.06 microns) as compared to CO_2 laser wavelength (10.6 microns) [Tu and Paleocrassas, 2020]. In a recent review of laser-based techniques for surface modification of Al alloys [Quazi et al, 2015], the techniques included laser surface melting, laser surface alloying, laser surface cladding, laser composite surfacing and laser shock peening. Of these, laser shock peening is closest to what is being used in the current project. Laser shock peening was reported to improve corrosion resistance in AA6082-T651 and AA2050-T8 alloys. In some specific alloy chemistries, corrosion resistance was enhanced and attributed to finely dispersed particles, metastable phases, and microstructural refinement. Surface alloying by elements such as Cr and Ni improved corrosion resistance while formation of phases, such as Al_4C_3 deteriorated it. Most recently at MS&T Conference 2020, R. Lavelle, et al. presented results for laser processing of several 5xxx and 6xxx series Al alloys and for different tempers (including 6061-T6). The authors concluded, based on visual pitting density, that laser passivation offers similar corrosion protection as compared to conversion coatings. However, they did not present long-term corrosion test data.

In summary, laser modification of Al alloys has been reported and the resulting improvement or degradation of corrosion resistance is dependent upon the specific alloy chemistry and laser processing conditions.

2.4 Literature on Laser Processing of Stainless Steels

300-series steels (such as 304 and 316 grade stainless) have good corrosion resistance in ambient environments due to a self-healing chromium oxide layer. In marine environments, although 316 is superior to 304, both can undergo corrosion (e.g. pitting and crevice corrosion) depending upon local conditions, such as temperature, where the self-passivating layer is unable to heal. For example, Cr-depleted grain boundaries due to welding or prior processing are anodic relative to grain interiors and lead to intergranular corrosion.

In a welded 304 SS, laser surface melting pre-treatment was reported to improve the corrosion resistance by the following mechanisms: (i) dissolving inclusions and homogenizing surface chemistry that improves pitting resistance, (ii) dissolving Cr-rich carbides that releases Cr back into the matrix such that it can resume forming protective oxide layer against intergranular corrosion, and (iii) increasing the fraction of the low-angle $\Sigma 1$ sub-grain boundaries that have low energy and improve resistance against sensitization and intergranular corrosion [Kaul et al., 2009]. Seleka and Pityana [2007] attributed improved pitting resistance of laser-melted 304 SS to the presence of retained delta-ferrite on account of rapid solidification that produced a duplex microstructure, i.e., retained delta ferrite + austenite, instead of single phase (austenite) in the base microstructure. In the case of 316 stainless steels, laser melting and solidification has been shown to provide greater corrosion resistance (to salt water) and was attributed to finer grains and (111) crystallographic orientation [Lin et al, 2019]. Improved corrosion resistance in laser processed 316 SS was also reported during exposure to biological environment (Hank's solution) and attributed to low-energy grain boundaries [Balla et al., 2018].

In summary, laser surface modification of stainless steels has been reported and appears to be generally favorable in terms of increasing their corrosion resistance.

3.0 Experimental Procedure

3.1 Test Materials and Coupons

Three commercially available alloy sheet metals, 6061 Al (T6 temper) (~1.58 mm thick), 316 SS (~1.45 mm thick), and a low-carbon (C) steel (~1.38 mm thick) were selected as test materials representative of those used in the marine energy industry. These were cut into 3" x 3" sized coupons and provided to our collaborator (University of Iowa) for LSP. Non-LSP samples served as the baseline to compare against the LSP samples.

3.2 Laser Surface Processing

LSP was performed using a Q-Switched Nd:YAG nanosecond laser (Spectra-Physics Quanta-Ray Lab-150, wavelength 1064 nm) with an energy per pulse on the order of several hundreds of mJ/pulse. The laser repetition rate was 10 pulses per second with a pulse duration of 6~8 ns. The samples were immersed in water during LSP and the laser scan head was rastered on the top surface of the sample to create a ~1" x 1" laser processed area. For each given material, individual LSP samples were fabricated corresponding to average laser power values of 0.9 W, 1.28 W, 1.78 W, 2.34 W and 3.12 W. Guided by the corrosion trend in low-C steel processed in 0.9 - 3.12 W range in initial part of this work (labeled as Batch #1), additional samples (labeled as Batch #2) were processed at "lower" laser powers of 0.3, 0.4 and 0.8 W and corrosion tested in the same manner as Batch #1.

3.3 Corrosion Testing

Although 316 SS and 6061 Al were expected to show some corrosion during long-term exposure to seawater, *short-term* corrosion experiments on these alloys did not show pitting or any other obvious signs of general corrosion. In order to make up for time lost due to COVID-19, we researched the literature to identify corrosion testing methods that could (i) potentially reveal different corrosion response from the LSP vs. the baseline samples and, (ii) enable such distinction within a "short" test duration (e.g., a week). Further, due to the limited number of LSP test coupons, a corrosion screening test was desired that could elucidate any impact of LSP parameters on corrosion behavior and thus distinguish the relative protection afforded by each of the selected laser processing conditions.

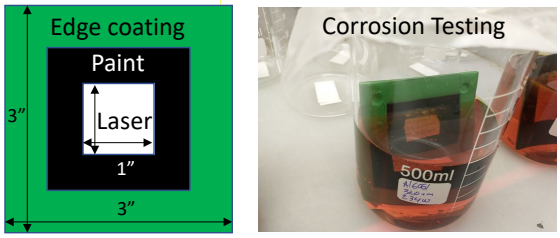

Figure 2: (a) Schematic of a LSP sample for corrosion testing. (b) Picture of a LSP sample dipped in ferric chloride solution for corrosion testing per ASTM G48 standard.

Accordingly, standard test method ASTM G48, typically used for testing the pitting and crevice corrosion resistance of materials to an oxidizing chloride environment, was selected to evaluate LSP and baseline samples of 316 SS and 6061 Al. A ferric chloride ($FeCl_3$) solution was prepared per ASTM G48 and the test samples were dipped in individual beakers. The samples

were taken out of the ferric chloride solution at regular intervals, washed, dried, weighed, and observed under a stereo microscope. Unlike 316 SS or 6061 Al, low-carbon steel has almost no corrosion resistance against seawater and rusts readily. Therefore, the corrosion behavior of LSP and baseline low-carbon steel was determined by dipping them into a 3.5 wt.% NaCl water instead of $FeCl_3$. Irrespective of the test material, the non-LSP portion of the material surrounding the 1" x 1" LSP region, was coated (see Fig. 2) to prevent it from interfering with the corrosion testing of the LSP region.

3.4 Surface Characterization

Test samples were imaged using a stereo optical microscope at identical magnification for a gross surface analysis of the corroded surface. Additionally, sample surface roughness was determined using a Bruker Contour GT-I optical profilometer operating in the Vertical Scanning Interferometry mode (0.1 nm vertical resolution). The vertical scanning range was set at 100 μm below the surface and 50 μm above the surface for the steel samples. The range was increased to 500 μm below the surface for the aluminum samples to include the deeper holes present in the corroded samples. The profilometer used a white light source, in conjunction with combinations of interferometric objectives and field-of-view lenses. Five regions, with no overlapping areas, were scanned on each sample and an average roughness (per sample) was computed in terms of root mean square roughness (Rq).

A limited set of Al samples were analyzed using X-ray photoelectron spectroscopy (XPS) utilizing a Thermo Fisher Nexsa spectrometer. This system uses a focused monochromatic Al Kα X-ray (1486.7 eV) source for excitation and a spherical section analyzer. The high energy resolution spectra were collected using a pass energy of 50 eV with a step size of 0.1 eV. For the Ag $3d_{5/2}$ line, these conditions produced a full-width half maximum (FWHM) of 0.82 eV ± 0.05 eV. The spectra were collected with an electron emission angle of 60° relative to surface normal. XPS depth profiles were performed using 3 kV monoatomic Ar+ ions rastered over 2 mm x 2 mm area of the sample surface. The corrected relative sputter rate on the Al samples was 0.097 nm/s (using a calibrated sputter rate of 0.21 nm/s on SiO_2 and an Al_2O_3/SiO_2 sputter ratio of 0.46). Thus, when the XPS data is plotted as a function of etch time, the depth within the sample at any etching instant is a product of the etching rate (0.097 nm/s) and the etching time.

4.0 Results

4.1 6061-T6 Al

Fig. 3 shows optical images of 6061-T6 Al samples that were subjected to an accelerated corrosion test (ASTM G48) using $FeCl_3$ as the corrosion solution. While the LSP surface of 6061 Al was whitish in color, immersion in $FeCl_3$ solution led to localized pitting corrosion that appears as small dark spots visible in the optical images. With increased immersion time from 1 hour to 2 hours, the samples (visually) appear to be more corroded. Although the optical images show an apparent greater pitting (i.e., more corrosion) in the LSP samples relative to the baseline, the sample weight (Fig. 4) shows a different trend.

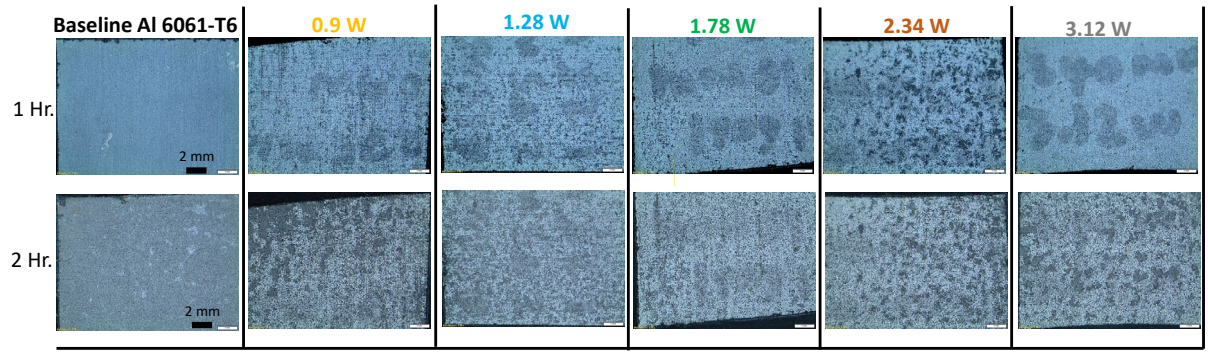

Figure 3: Optical microscope images of Al 6061-T6 samples following accelerated corrosion test in $FeCl_3$ solution at room-temperature for 1 hour (top row) and 2 hours (bottom row). The samples are arranged (left -to-right) in the order of increasing laser power used for LSP listed at the top of each column. Baseline (1st column) refers to non-LSP samples.

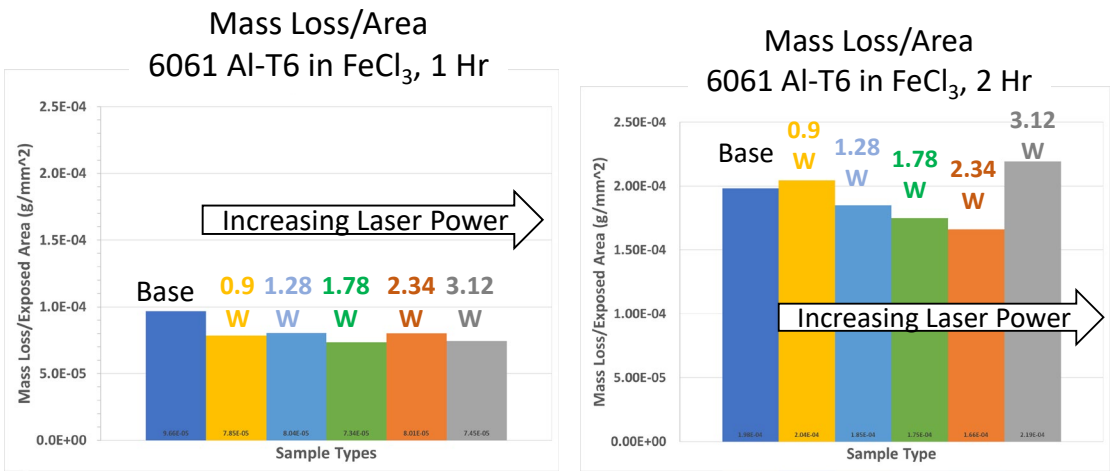

Figure 4: Mass loss per unit corrosion exposed area of 6061-T6 Al in baseline samples and after LSP. A higher mass-loss is indicative of greater corrosion of the material. Laser power (in Watts) for a given LSP sample is listed above its corresponding data bar.

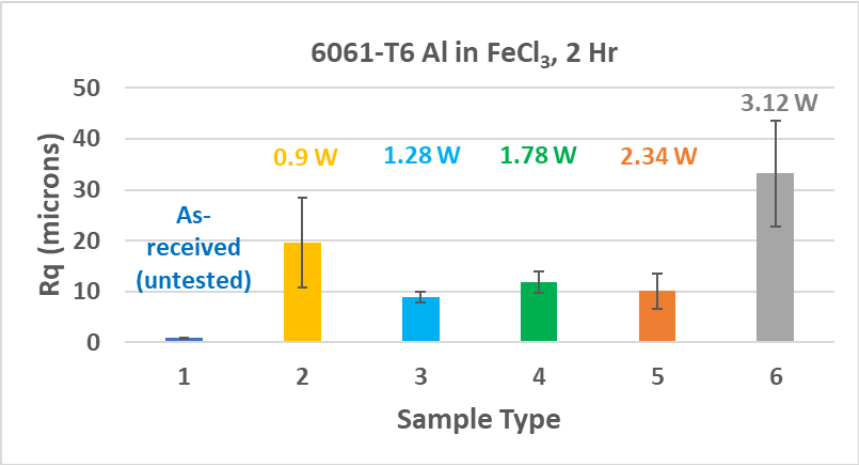

Figure 5: Root mean square deviation of the profile (Rq) of 6061-T6 Al in the as-received (untested) and in LSP + corrosion tested samples. Laser power (in Watts) for a given LSP sample is listed above its corresponding data bar and the error bars represent the standard deviations of five measurements for each sample.

Fig. 4 shows the mass loss per unit area for each of the 6061 Al samples after 1 hour and 2 hours corrosion testing. The data shows that after 1 hour, the LSP samples show up to ~23% lower mass loss relative to the baseline. However, after 2 hours testing, a clear trend emerges as a function of laser power: The lowest (0.9 W) and the highest power (3.12 W) LSP samples show greater corrosion than the baseline, while the intermediate power samples (1.28, 1.78 and 2.34 W) show lower corrosion than the baseline with the lowest corrosion (~16%) shown by the 2.34 W LSP sample. The lower corrosion in the middle-power range of LSP samples (i.e., 1.28, 1.78 and 2.34 W laser processed) is also accompanied by relatively lower roughness, as shown in Fig. 5. Slow corroding samples seem to retain their low, original roughness from the as-received state while the faster corroding samples seem to develop an uneven surface and hence, a rougher profile. **This lower corrosion, for a selected range of laser power, confirms our original hypothesis of improved corrosion resistance through LSP and the need to optimize LSP conditions for optimum corrosion resistance.**

Fig. 6 shows the depth profile of near-surface chemical composition, obtained using the XPS technique, in (a) unprocessed Al and (b) LSP + corrosion tested Al (2.34 W). In the unprocessed Al, the Al concentration signal rapidly increases to ~100% while that of O simultaneously decreases to 0, indicative of a thin native oxide layer. This oxide layer is estimated to be ~400 nm thick based on the decay of the concentration vs. etch time curve. By comparison, the Al signal in LSP + corrosion tested sample initially rises to ~35 at.% followed by a gradual increase to ~55% at ~1 μm depth. Simultaneously, the O content is ~60 at.% near the surface, decreasing to ~45 at.% at ~1 μm depth. In other words, this sample also seems to have some sort of an aluminum oxide (or possibly oxide + hydroxide) layer but one that is at least ~1 μm thick (based on the non-zero value of oxygen signal even after 10,000 s of etching).

Fig. 7 shows the evolution of Al 2p spectra at several different XPS sputtering cycles, i.e., as a function of depth into the LSP + corrosion tested sample. The data show a near-surface peak at ~74.5 eV (Cycle #6) that can be ascribed to Al-O bonding and supporting the idea of an

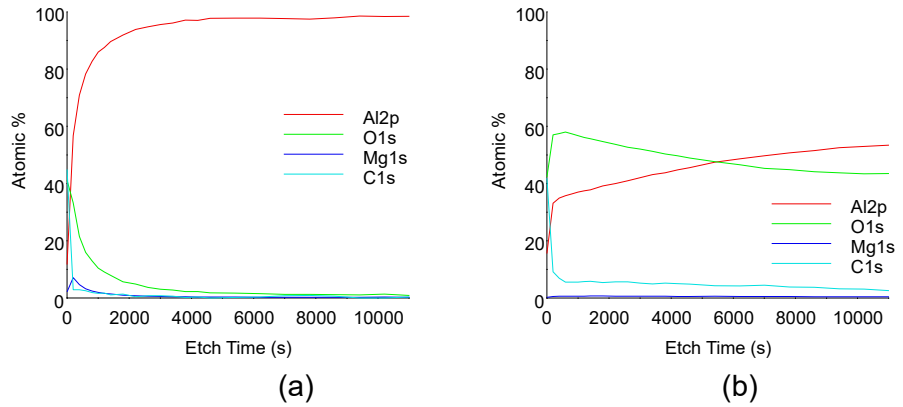

Figure 6: Near-surface chemical composition determined using XPS depth-profiling in (a) untested 6061-T6 Al and (b) LSP + corrosion tested 6061-T6 Al (2.34 W, 2 hr. test).

aluminum oxide layer. With further sputtering, the Al-O peak decreases while another peak at ~73 eV is visible (Cycle #'s 12, 18 and 23). The peak at ~73 eV is associated with metallic Al indicating that the oxide layer is gradually transitioning to the un-modified base metallic Al.

Thus, the XPS (Fig. 6-7) and corrosion data (Fig. 4) together suggest that LSP produces an aluminum oxide layer on the surface that seems to be lowering the corrosion rate in the LSP Al relative to unprocessed Al. It is noted that LSP may have also modified the sub-surface microstructure to be more corrosion resistant and requires additional microstructural analysis to distinguish the roles of the microstructure and the surface oxide.

4.2 Low-carbon Steel *(Batch #1)*

Fig. 8 shows optical images of low-carbon steel samples that were subjected to corrosion tests in a 3.5% NaCl solution at room-temperature. The LSP'ed surface was whitish in color that got increasingly covered in rust with increasing immersion time. Fig. 9 shows the mass loss per unit area for each of the samples after 4 hours and 24 hours corrosion testing, and unlike Al

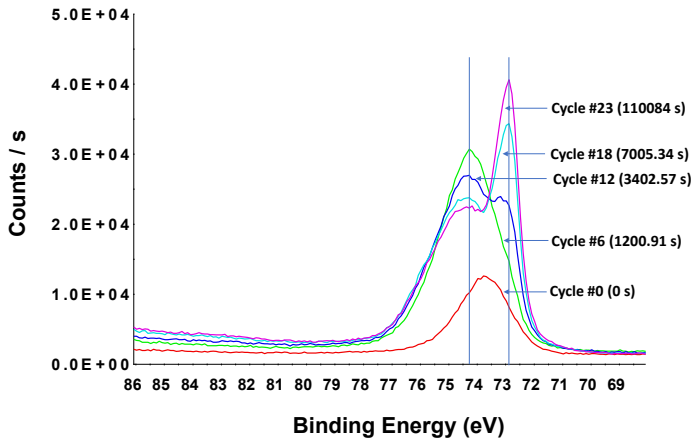

Figure 7: Al 2p XPS spectra of the LSP + corrosion tested (2 hr.) 6061-T6 Al.

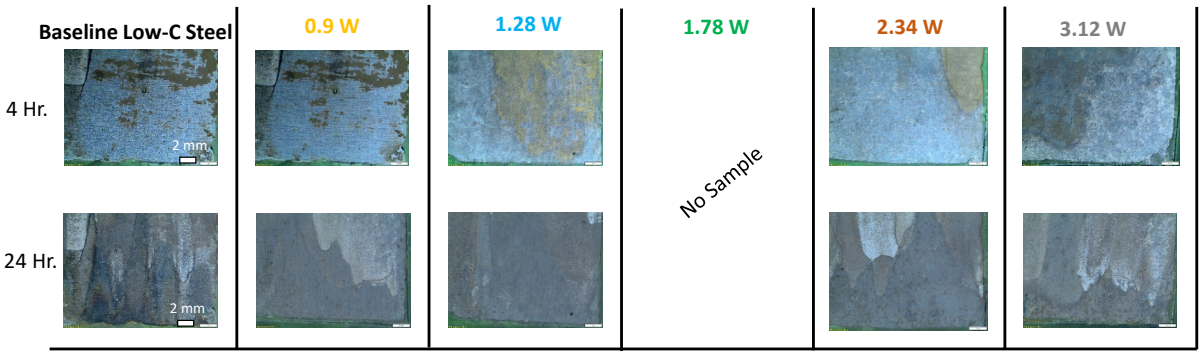

Figure 8: Optical microscope images of a low-carbon steel samples (Batch #1)following corrosion test in 3.5% NaCl solution at room-temperature for 4 hours (top row) and 24 hours (bottom row). The samples are arranged (left -to-right) in the order of increasing laser power used for LSP listed at the top of each column. Baseline (1st column) refers to non-LSP samples.

samples (Fig. 4), all of the LSP samples showed a greater mass loss (i.e., more corrosion) than the baseline sample. **The data also shows that the lowest laser power (0.9 W) was closest in its performance to baseline sample suggesting that perhaps an even lower laser power (i.e., < 0.9 W) may be able to improve this steel's corrosion resistance.** As described subsequently, this hypothesis was verified in Batch #2 samples processed with laser power < 0.9 W.

Fig. 10 shows the surface roughness of low-C steel samples in different test conditions and unlike corrosion tested 6061-Al samples (Fig. 5), lower relative corrosion in low-C steel is not associated with lower values of Rq. It is possible that the rust layer on corroded steel samples (Fig. 8) produces a relatively smooth surface on all the samples such that the roughness can no longer be related to extent of corrosion. Relative smoothness of corroded surface in steel samples is also indicated by the magnitude (~1-1.1 μm) unlike ~10-40 μm in 6061-Al (Fig. 5).

4.3 Low-carbon Steel *(Batch #2)*

Figs. 11 and 12 show optical images and mass loss per unit area, respectively, for the low-C steel samples (Batch #2) following 8 hr. and 24 hr. testing in 3.5% NaCl solution at room-

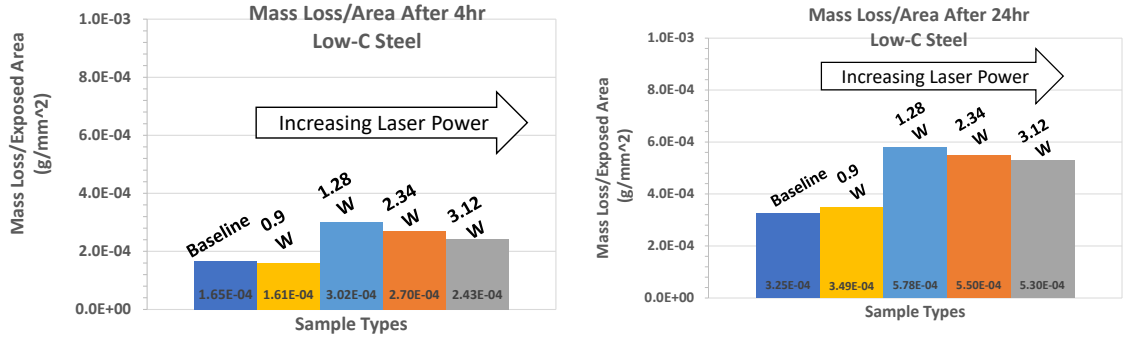

Figure 9: Mass loss per unit corrosion exposed area of low-carbon steel (Batch #1) in baseline samples and after LSP. A higher mass-loss is indicative of greater corrosion of the material. Laser power (in Watts) for a given LSP sample is listed above its corresponding data bar.

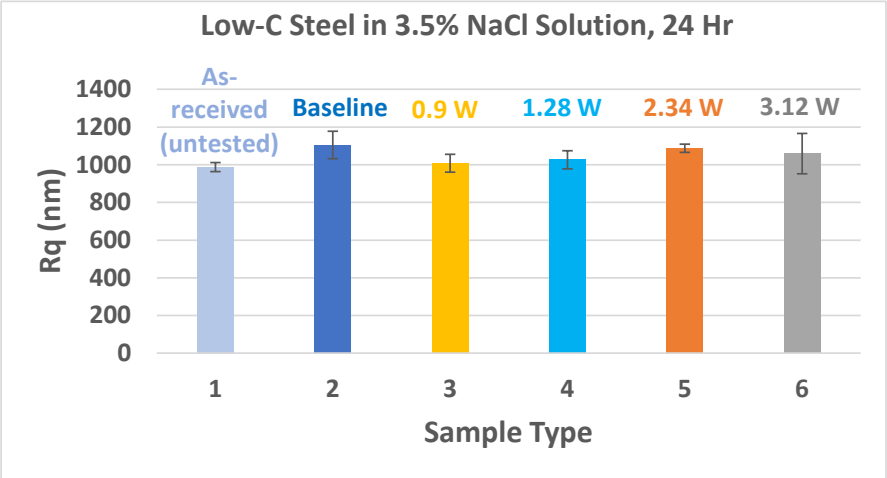

Figure 10: Root mean square deviation of the profile (Rq) of low-carbon steel (Batch #1) in the as-received (untested), baseline (as-received + corrosion tested) states, and in LSP + corrosion tested states. Laser power (in Watts) for a given LSP sample is listed above its corresponding data bar and the error bars represent the standard deviations of five measurements for each sample.

temperature, similar to Batch #1 corrosion tests. While the two steel batches have a generally similar appearance after corrosion testing, Fig. 12 shows that Batch #2 samples underwent *lower* corrosion than the baseline sample. In fact, the corrosion mass loss in 0.8 W sample was ~25% lower than the baseline. **Therefore, the data in Fig. 12 confirms the hypothesis that there may be a threshold laser power below which the corrosion resistance of laser processed low-C steel could be improved**.

Since the low-C steel used in the current work doesn't contain any appreciable alloying elements, an alloy oxide-hydroxide layer, such as that observed in LSP Mg alloy [Jana et al., 2021], is not expected in the present case. Therefore, it is conjectured that in the case of low-C steel, laser-induced sub-surface microstructural changes (e.g., grain-size, grain boundary nature, dislocation density, etc.) may be playing a role in its corrosion behavior. A detailed

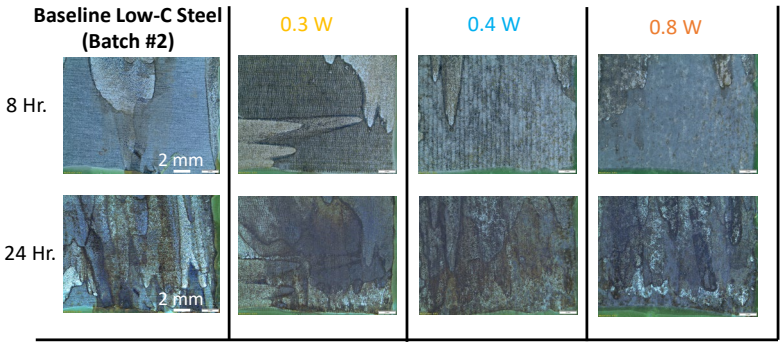

Figure 11: Optical microscope images of a low-carbon steel samples (Batch #2) following corrosion test in 3.5% NaCl solution at room-temperature for 8 hours (top row) and 24 hours (bottom row). The samples are arranged (left -to-right) in the order of increasing laser power used for LSP listed at the top of each column. Baseline (1st column) refers to non-LSP samples.

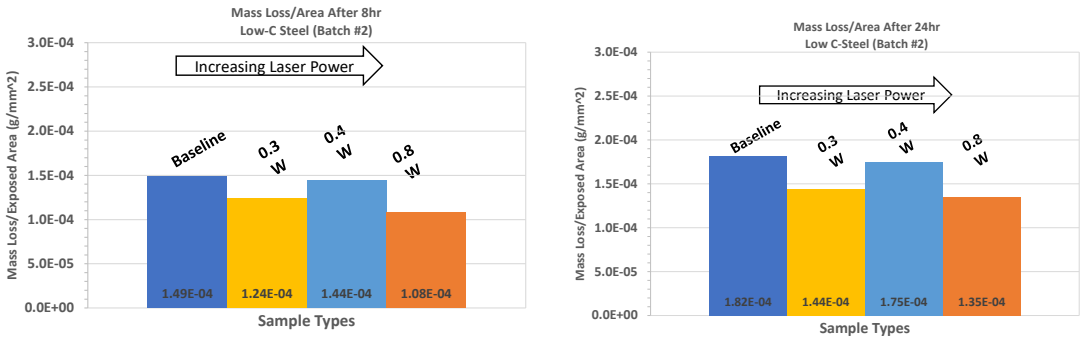

Figure 12: Mass loss per unit corrosion exposed area of low-C steel (Batch #2) in baseline samples and after LSP. A higher mass-loss is indicative of greater corrosion of the material. Laser power (in Watts) for a given LSP sample is listed above its corresponding data bar.

microstructural analysis is proposed for future work to understand the reason(s) for the difference in corrosion performance at low (< 0.9 W) vs. high (> 0.9 W) laser power. Additionally, studies with multiple samples per laser processing condition, in sea-water conditions, and for longer duration, would also be useful for a better understanding and validating the beneficial effects of laser processing on low-C steel.

4.4 316 Stainless Steel

Preliminary accelerated corrosion tests on the baseline 316 SS (i.e., without LSP) in a $FeCl_3$ solution (per ASTM G48 standard) did not show any visual indications of pitting even after a week (168 hours) of testing. Therefore, corrosion test duration longer than a week seems necessary to initiate pitting corrosion and enable comparison of LSP vs non-LSP 316 SS. This steel is also known to undergo crevice corrosion, which can be more severe than general or pitting corrosion and can occur in mechanical joints (e.g., in bolted joints) common in marine energy devices (especially tidal and current turbines). However, crevice corrosion testing requires additional experimental preparation beyond the scope of the current Seedling.

5.0 Summary & Conclusions

Corrosion in marine environments is unavoidable and an expensive problem that is typically addressed by coatings and paints. Surface modification techniques for corrosion protection, including those involving lasers, have been researched to some extent, more so in steels than in Al alloys. Such research is at low TRL and suggests improvement in corrosion resistance in selective, lab-scale tests. However, corrosion resistance in longer-term and real-world environments needs to be demonstrated. Although laser raster speed can be on the order of m/s, the laser-modified surface region is limited by the laser spot size that is typically < mm in diameter. This limited areal coverage of the laser beam suggests that laser-based approaches may be more relevant for selective area modifications (e.g., near welds, joints, etc.) or on small-sized components, while their applicability to modify very large area structures (e.g., beams, pillars, plates, etc.) will be limited unless systems with extremely fast rastering speed can be developed.

Under the testing conditions employed here, the main conclusions of this Seedling project are:

1. LSP of 6061-T6 Al shows up to ~15% improved corrosion resistance, relative to baseline, under accelerated corrosion tests. Preliminary surface analysis through XPS suggests that LSP produces an aluminum oxide layer on the surface that seems to be lowering the corrosion rate in the LSP Al relative to unprocessed Al. Additional work is necessary to distinguish the roles of the microstructure and the surface oxide in improving corrosion resistance (in LSP samples) and to translate the accelerated test data to long-term corrosion under realistic marine conditions.

2. LSP of low-C steel shows up to ~25% improved corrosion resistance, relative to baseline, in 3.5% saline solution. There appears to be a threshold average laser power (~0.9 W) below which laser processed low-C steel shows improved corrosion resistance but is worse above the threshold. Additional work is necessary to understand how the underlying microstructure (and hence, the corrosion behavior) changes below/above the threshold laser power.

3. Lower surface roughness (after corrosion testing) was associated with lower corrosion (and vice-versa) in LSP 6061-T6 Al, while the two were relatively independent in the case of low-carbon steel. The different behavior in Al and steel can be attributed to pitting type corrosion in Al as opposed to the formation of a rust layer in steel.

4. LSP effects on corrosion resistance of 316 SS could not be determined in the current Seedling – This steel intrinsically has a relatively good corrosion resistance and therefore, did not show pitting within the short-duration tests. Hence, longer-term corrosion tests are necessary to evaluate LSP's effects on corrosion resistance; crevice corrosion tests might be suitable to determine LSP's efficacy in short-duration corrosion tests.

6.0 Proposed Future Steps

Corrosion in marine environments is a significant challenge and low-cost surface protection technologies are needed for greater penetration of marine energy sources. We propose that efforts be made to identify and understand corrosion protection mechanisms in laser modified steel and Al alloys and to evaluate the efficacy of such modified surfaces in long-term tests and in variety of corrosion environments. Use of LSP in local regions, such as at joints and welds, of components and structures should be explored. In parallel efforts, we propose that this knowledge be used to develop non-laser methods (e.g., heat-treatments, benign/environmentally friendly chemical techniques) that take advantage of same or similar protection mechanisms as laser techniques but can process larger structures as well (e.g., pillars, beams etc.) used in marine energy applications.

7.0 References

ASM International Handbook: https://dl.asminternational.org/handbooks/book/26/chapter/355416/Corrosion-in-the-Military

Balla, V.K., Dey, S., Muthuchamy, A.A., Janaki Ram, G.D., Das, M., and Bandyopadhyay A. Laser surface modification of 316L stainless steel. Journal of Biomedical Materials Research B: Applied Biomaterials Feb (2018), Vol. 106B, Issue 2, pp. 569-577.

GAO Report: https://www.govinfo.gov/content/pkg/GAOREPORTS-GAO-03-753/html/GAOREPORTS-GAO-03-753.htm, accessed 1/1/2021.

Jana, S., M. Olszta, D. Edwards, M. H. Engelhard, A. Samanta, H. Ding, P. Murkute, O. B. Isgor, and A. Rohatgi, "Microstructural Basis for Improved Corrosion Resistance of Laser Surface Processed AZ31 Mg Alloy" Corrosion Science (2021) 191, 109707 10.1016/j.corsci.2021.109707

Kaul, R., Parvathavarthini, N., Ganesh, P., Mulki, S.V., Samajdar, I., Dayal, R.K., and Kukreja, L.M. A Novel Preweld Laser Surface Treatment for Enhanced Intergranular Corrosion Resistance of Austenitic Stainless Steel Weldments. Supplement to the Welding Journal, December 2009, pp. 233-242.

Lavell, R., Rearick, D., Klingenberg, M., Snyder, D., Fox, J., Witt, A., and Oneil, T. Laser Ablation and Passivation of Al Alloys. Presented at MST 2020 on-line conference.

Lin, K., Gu, D., Xi, L. Yuan, L., Niu, S., Lv, P., and Ge, Q. Selective laser melting processing of 316L stainless steel: effect of microstructural differences along building direction on corrosion behavior. The International Journal of Advanced Manufacturing Technology (2019) 104:2669–2679.

News Report: https://www.military.com/daily-news/2020/01/13/battle-against-rust-3-billion-problem-navy.html, accessed 7/22/2020.

ONR Departments: https://www.onr.navy.mil/en/Science-Technology/Departments/Code-33/All-Programs/333-weapons-and-payloads/corrosion-control

Popular Mechanics article: https://www.popularmechanics.com/military/navy-ships/a30522792/navy-fighting-rust/, accessed 1/16/2020.

Quazi, Moumin, Fazal, Md Abul, Haseeb, Ahmed, Farazila, Yusof, Masjuki, Haji Hassan, and Arslan, Arslan. Laser-based Surface Modifications of Aluminum and its Alloys. Critical Reviews in Solid State and Materials Sciences, 0:1–26, 2015, DOI: 10.1080/10408436.2015.1076716.

Seleka, Tshidiso and Pityana, Sisa. Laser surface melting of 304 stainless steel for pitting corrosion resistance improvement. The Journal of the Southern African Institute of Mining and Metallurgy, 107, 2007, pp. 151-154.

Tu, F. Jay and Paleocrassas, G. Alexander. Low speed laser welding of aluminum alloys using single-mode fiber lasers. Laser Welding, Xiaodong Na, Stone (Ed.), ISBN: 978-953-307-129-9, InTech, 2020, pp. 47-76.

VCI Inhibitors: https://www.cortecvci.com/Publications/Papers/Military/MILNACE01.html , accessed 1/1/21.

Pacific Northwest National Laboratory

902 Battelle Boulevard
P.O. Box 999
Richland, WA 99354
1-888-375-PNNL (7665)

www.pnnl.gov